

## Origin of the anomalous magnetic behavior of the $\text{Fe}_{13}^+$ cluster

M. Wu,<sup>1</sup> A. K. Kandalam,<sup>2</sup> G. L. Gutsev,<sup>3</sup> and P. Jena<sup>1,\*</sup>

<sup>1</sup>*Department of Physics, Virginia Commonwealth University, Richmond, Virginia 23284, USA*

<sup>2</sup>*Department of Physics, West Chester University, West Chester, Pennsylvania 19383, USA*

<sup>3</sup>*Department of Physics, Florida A&M University, Tallahassee, Florida 32307, USA*

(Received 26 April 2012; revised manuscript received 19 September 2012; published 12 November 2012)

By using density functional theory, we show that the exceptionally low value of the total magnetic moment of  $\text{Fe}_{13}^+$  observed in an experiment [*Phys. Rev. Lett.* **108**, 057201 (2012)] is not due to antiferromagnetic coupling between the spins of the core and surface atoms as hypothesized but is due to the symmetry-driven quenching of the local spin moments of all atoms with the largest quenching observed for the central atom. Our study of  $\text{Fe}_{12}^+$ ,  $\text{Fe}_{13}^+$ ,  $\text{Fe}_{14}^+$ , and their neutral parents reveals that the total magnetic moment of  $\text{Fe}_{13}^+$  decreases by  $9\mu_B$  with respect to that of neutral  $\text{Fe}_{13}$ , whereas, the changes are  $1\mu_B$  and  $3\mu_B$  for  $\text{Fe}_{12}^+$  and  $\text{Fe}_{14}^+$ , respectively.

DOI: [10.1103/PhysRevB.86.174410](https://doi.org/10.1103/PhysRevB.86.174410)

PACS number(s): 75.75.-c, 36.40.Wa, 36.40.Cg, 36.40.Mr

The importance of magnets in technology and society has been a driving factor in the search for new magnetic materials with improved functionality. Two quantities are of primary interest in this search: magnetic moment per atom and the nature of coupling between these moments. Since these can be tailored by varying the size, symmetry, and dimensionality of materials,<sup>1</sup> in the last few years, much attention has focused on the study of magnetism in transition-metal clusters<sup>2–13</sup> where the size and composition can be controlled one atom at a time. It has been predicted theoretically<sup>2–7</sup> and has been verified experimentally<sup>8–10</sup> that clusters of nonmagnetic elements, such as Ti, V, Rh, and Pd can become magnetic, whereas, the magnetic moments per atom of Fe, Co, and Ni clusters exceed their respective values in the bulk phase.<sup>11–13</sup> Furthermore, these moments nonmonotonically decrease with size, eventually reaching the bulk limit in clusters containing about 1000 atoms.

Early experimental studies of magnetism in transition-metal clusters were performed using the Stern-Gerlach technique,<sup>8–13</sup> which cannot distinguish between contributions from the orbital and spin moments to the total magnetic moment  $L + 2S$ . Although the orbital moments are known to be quite small in crystals, they are usually<sup>14,15</sup> much larger in clusters. In a recent x-ray magnetic circular dichroism experiment, Niemeyer *et al.*<sup>16</sup> have separated the orbital and spin magnetic moments of the positively charged  $\text{Fe}_n^+$  ( $n = 2–20$ ) clusters. The total magnetic moment per atom exhibits a nearly monotonous growth as a function of  $n$ , except for  $n = 13$ , where the total magnetic moment per atom drops to an exceptionally low value of  $2.4 \pm 0.4\mu_B$ . Since the orbital magnetic moments are nearly constant across the series and do not exceed  $\sim 0.4\mu_B$ , the above anomaly can only originate from the reduced spin contribution to the total magnetic moment. Niemeyer *et al.*<sup>16</sup> explained this deviation by comparing their finding with the results of computations performed for the neutral  $\text{Fe}_{13}$  cluster. If one accepts a one-electron model where the electron detaches from a spin-up or spin-down occupied orbital without significant reconstruction of the rest of the orbitals, then the total magnetic moment of a cluster would change by  $\pm 1.0\mu_B$ . This is indeed the case in the  $\text{Fe}_2$ - $\text{Fe}_6$  series,<sup>17,18</sup> except for  $\text{Fe}_4^+$ , whose total magnetic moment is smaller by  $3.0\mu_B$  than that of neutral  $\text{Fe}_4$ . The total magnetic moment of  $\text{Fe}_{13}^+$ , on

the other hand, is quenched by  $9.0\mu_B$  with respect to that of its neutral parent. Niemeyer *et al.*<sup>16</sup> suggested that this anomalous result could be due to the antiferromagnetic coupling between the magnetic moments of the central atom and the surface atoms since a state possessing such a coupling was found<sup>19</sup> to have a total magnetic moment of  $34\mu_B$  in the neutral  $\text{Fe}_{13}$  cluster. If one accepts such an explanation, then the next question would be why similar quenching of the total magnetic moment is not observed in the neighbors  $\text{Fe}_{12}^+$  and  $\text{Fe}_{14}^+$  whose neutral parents possess quite similar geometric structures resulting from adding ( $\text{Fe}_{14}$ ) or removing ( $\text{Fe}_{12}$ ) a Fe atom to/from a nearly icosahedral geometrical configuration of  $\text{Fe}_{13}$ .<sup>20–22</sup>

To understand this anomalous behavior, we performed a first-principles theoretical study of the structural and magnetic properties of neutral and singly positively charged  $\text{Fe}_n$  clusters with  $n = 12, 13$ , and  $14$ . Although neutral  $\text{Fe}_n$  clusters of this size were the subject of several theoretical papers,<sup>20–24</sup> no computational results were reported on singly positively charged iron clusters in this size range. Our calculations are performed using density functional theory with generalized gradient approximation (GGA) for the exchange and correlation potentials. In order to examine the sensitivity of our results to the choice of basis sets and GGA functionals, we have used three computational methods that employ different basis sets: the Vienna *ab initio* simulation package<sup>25</sup> (VASP) with the plane-wave basis,<sup>26</sup> DMOL<sup>3</sup> (Ref. 26) with a numerical basis, and GAUSSIAN 09 (Ref. 27) with the Gaussian basis functions. In our VASP computations, we used the projector augmented wave method<sup>28</sup> where the kinetic-energy cutoff, convergence of total energy, and convergence of forces were set to 500, 0.0001 eV, and 0.01 eV/Å, respectively. In our DMOL<sup>3</sup> computations, an all-electron double numerical basis set, extended with polarization functions, was used, the real-space global cutoff radius was set to 4.6 Å, and optimizations were performed until the forces on all atoms became smaller than 0.005 eV/Å. In our G09 calculations, we used the 6–311+G\* basis set,<sup>29</sup> ultrafine integration grids, and G09 default optimization criteria. The exchange-correlation functionals used were the BPW91 (composed from the Becke exchange<sup>30</sup> and Perdew-Wang correlation<sup>31</sup>), the PW91 (Ref. 32), and the Perdew-Burke-Ernzerhof (PBE) (Ref. 33).

TABLE I. Total spin magnetic moments (in  $\mu_B$ ) of the lowest total energy isomers of  $Fe_n$  and  $Fe_n^+$  clusters obtained by using different codes and exchange-correlation functionals. The experimental values of the magnetic moments per atom in  $Fe_{12}^+$ ,  $Fe_{13}^+$ , and  $Fe_{14}^+$  are  $3.41 \pm 0.50\mu_B$ ,  $2.44 \pm 0.38\mu_B$ , and  $3.49 \pm 0.48\mu_B$ , respectively.

Cluster	VASP	VASP	DMOL <sup>3</sup>	GAUSSIAN 09
	PBE	PW91	PW91	BPW91
$Fe_{12}$	36	36	38	36
$Fe_{12}^+$	37	37	37	37
$Fe_{13}$	44	44	42	44
$Fe_{13}^+$	35	35	35	35
$Fe_{14}$	46	44	46	46
$Fe_{14}^+$	43	43	43	43

To obtain the ground-state geometries of both the neutral and the positively charged  $Fe_n$  ( $n = 12-14$ ) clusters, we started with geometric configurations of isomers previously investigated for the neutral clusters. The geometries of the positively charged clusters were obtained by optimizing the geometries of the neutral isomer states with one electron removed. Each geometry optimization was followed by harmonic vibrational frequency computations in order to confirm the stationary character of the state obtained. The states with icosahedral-type geometries were found to be well separated from other isomers as was previously found for the neutral  $Fe_{13}$  cluster.<sup>19,20</sup> All three approaches are found to produce similar geometric structures for the lowest total energy states of both neutral and positively charged iron clusters. The spin magnetic moment is computed as  $2S = n_\alpha - n_\beta$ , where  $n_\alpha$  and  $n_\beta$  are the numbers of the spin-up and spin-down electrons, respectively. We accept the local magnetic moments on atoms to be equal to the excess spin density obtained using the Mulliken or natural atomic orbital (NAO) populations. Table I presents the total magnetic moments obtained by the three different methods. The moments had small variations in the neutral series depending on the method or functional used, whereas, all approaches arrived at the same values for the  $Fe_{12}^+$ ,  $Fe_{13}^+$ , and  $Fe_{14}^+$  cations. To validate our computational approach, we have calculated the vertical ionization energies of the neutral  $Fe_n$  clusters as the difference in total energies of the neutral ground states and the cations at their respective neutral equilibrium geometries. The vertical ionization potentials obtained using the GAUSSIAN 09 code are 5.33, 5.62, and 5.63 eV for  $n = 12-14$ , respectively, and agree well with two series of the experimental values:  $5.42 \pm 0.16$ ,  $5.76 \pm 0.18$ , and  $5.80 \pm 0.19$  (Ref. 34) and  $5.52 \pm 0.05$ ,  $5.61 \pm 0.05$ , and  $5.70 \pm 0.05$  eV,<sup>35</sup> respectively.

Geometries of the ground-state and some higher-energy isomers of neutral and cationic  $Fe_n$  ( $n = 12-14$ ) clusters are shown in Figs. 1-3. We begin with Fig. 1 where geometrical configurations of  $Fe_{13}$  and  $Fe_{13}^+$  corresponding to the lowest total energy state and isomers corresponding to the antiferromagnetic states are shown. For the latter, the local magnetic moments of one or two atoms are antiferromagnetically coupled to those of the rest of the atoms (the BPW91/6-311+G\* results). The magnetic moment of  $2.2\mu_B$  at the central atom in the neutral  $Fe_{13}$  ground state ( $2S = 44\mu_B$ ) is almost quenched in the  $Fe_{13}^+$  ground state. This is further

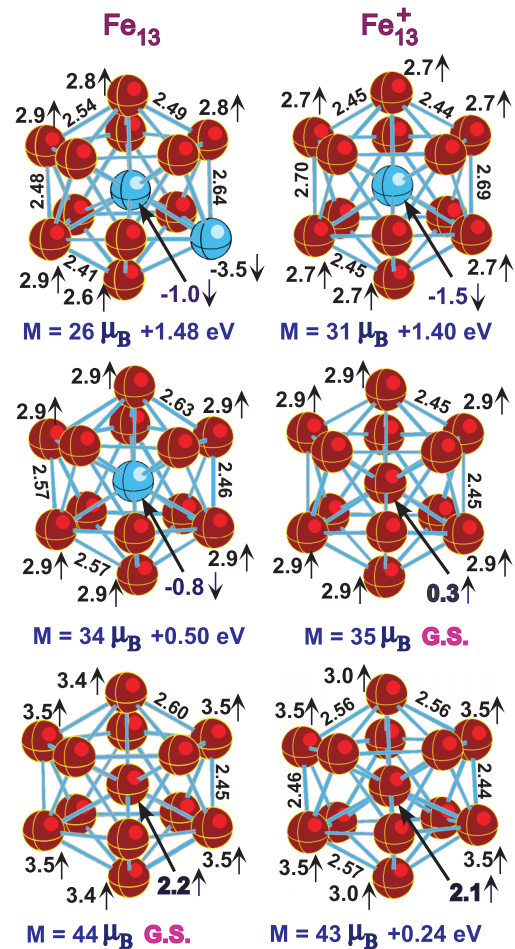


FIG. 1. (Color online) Geometries of the lowest total energy state and two antiferromagnetic states of  $Fe_{13}$  and  $Fe_{13}^+$ . Bond lengths are in angstroms, local magnetic moments are in  $\mu_B$ , and G.S. denotes the ground state. The blue (light) color is used for the atoms whose local spin magnetic moments are antiferromagnetically coupled to the local spin magnetic moments of atoms marked with the red (dark) color.

accompanied by a reduction in the magnetic moments of the surface atom of the ionized cluster. The cation states expected on the basis of the one-electron model ( $2S \rightarrow 2S \pm 1$ ) are higher in total energy than the ground state with  $2S = 35\mu_B$  by 0.32 eV ( $2S = 45\mu_B$ ) and 0.24 eV ( $2S = 43\mu_B$ , shown in Fig. 1). The cation  $Fe_{13}^+$  states with  $2S = 41\mu_B$ ,  $39\mu_B$ , and  $37\mu_B$  are above the ground state by 0.05, 0.02, and 0.02 eV, respectively, whereas, the sharp increase in total energy is found for the states with the total magnetic moments smaller than  $2S = 35\mu_B$  and larger than  $2S = 45\mu_B$  (see Fig. 4). Our total spin magnetic moment per atom in the lowest total energy state of  $Fe_{13}^+$  is  $2.69\mu_B$ , which agrees well with the experimental estimate of  $2.4 \pm 0.4\mu_B$ .<sup>16</sup>

According to our results for the  $Fe_{12}$ - $Fe_{12}^+$  pair presented in Fig. 2, no such anomaly as seen in the  $Fe_{13}$ - $Fe_{13}^+$  pair is observed. The lowest total energy state of the cation possesses  $2S = 37\mu_B$  and the state with  $2S = 35\mu_B$  is higher by 0.02 eV. Note that both these states are consistent with the one-electron model. The states with the total spin magnetic

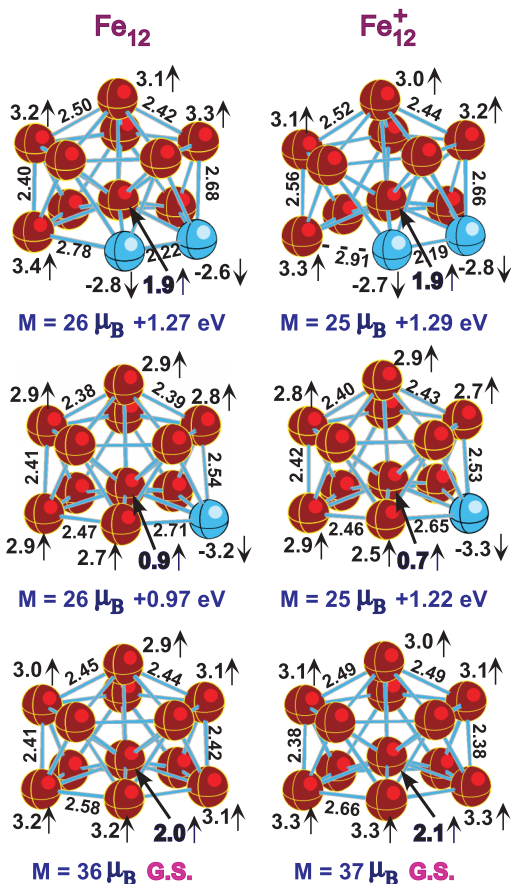


FIG. 2. (Color online) Geometries of the ground states of  $\text{Fe}_{12}$  and  $\text{Fe}_{12}^+$  and their states where the magnetic moment of the central atom is antiferromagnetically coupled to the magnetic moments of the surface atoms. The blue (light) color is used for the atoms whose local spin magnetic moments are antiferromagnetically coupled to the local spin magnetic moments of atoms marked with the red (dark) color.

moments of  $33\mu_B$  and  $39\mu_B$  are higher by 0.11 and 0.45 eV, respectively. There is a large difference of  $8\mu_B$  between the total spin magnetic moments of the lowest total energy states of neutral  $\text{Fe}_{12}$  and  $\text{Fe}_{13}$ . The Stern-Gerlach experimental data<sup>36</sup> showed unusually large total magnetic moments per atom exceeding  $5\mu_B$  for this size of neutral iron clusters. Niemeyer *et al.*<sup>16</sup> found that the orbital magnetic moment does not exceed 5%–15% of the total magnetic moment in the corresponding iron cations, and there is no reason to expect that this contribution would increase to  $\sim 50\%$  in the neutral iron clusters. Our total spin magnetic moment per atom in  $\text{Fe}_{12}^+$  is  $3.08\mu_B$ , which fits the experimental value of  $3.4 \pm 0.5\mu_B$  (Ref. 16) within the experimental error bars.

The total spin magnetic moment of  $\text{Fe}_{14}$  in its lowest total energy state is larger than that of  $\text{Fe}_{13}$  by  $2\mu_B$ . As is seen from Fig. 3, the isomer with a Fe atom attached to a face of  $\text{Fe}_{13}$  is higher in total energy by 0.48 eV than the lowest energy state where the additional atom participates in the formation of a hexagonal ring. In both isomers, the surface atoms possess similar magnetic moments of  $3.3\text{--}3.4\mu_B$ , whereas, the central atom carries a reduced magnetic moment. The

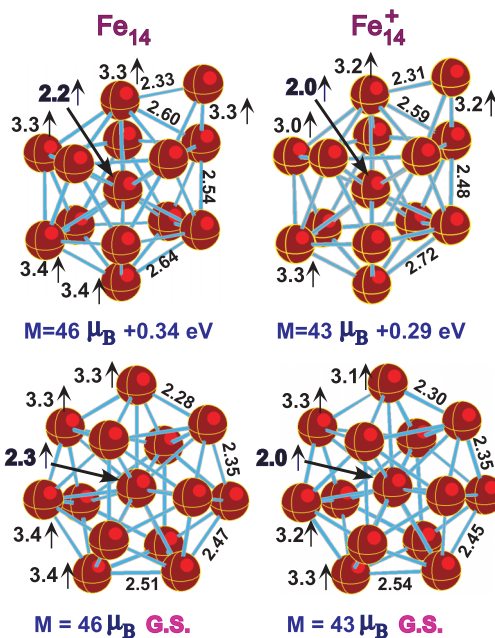


FIG. 3. (Color online) Geometries of two isomers of  $\text{Fe}_{14}$  and  $\text{Fe}_{14}^+$ .

electron detachment reduces the total magnetic moment by  $3\mu_B$ , without quenching the magnetic moment of the central atom in both isomers. The total energy behavior as a function of the total magnetic moment of  $\text{Fe}_{14}^+$  given in Fig. 4 is different from that in  $\text{Fe}_{13}^+$ . Although the total energy of the state with  $2S = 41\mu_B$  is higher than that of the lowest-energy state by 0.01 eV, the states with  $2S = 39\mu_B$  and  $45\mu_B$  are higher by 0.20 and 0.10 eV, respectively. The total spin magnetic moment per atom in the lowest total energy state of  $\text{Fe}_{14}^+$  is  $3.07\mu_B$ , which nearly matches the lower bound of the experimental value of  $3.5 \pm 0.5\mu_B$ .

In order to gain insight into the anomalous behavior of the total magnetic moment in  $\text{Fe}_{13}^+$ , we analyze the NAO

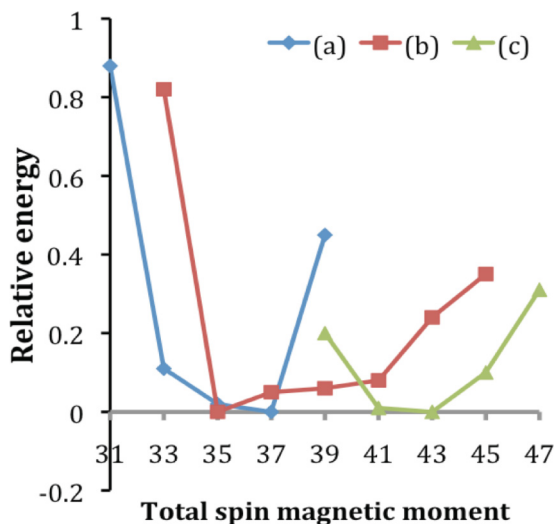


FIG. 4. (Color online) Total energy (relative to the corresponding ground-state total energy in eV) as a function of the total spin magnetic moment (in  $\mu_B$ ): (a)  $\text{Fe}_{12}^+$ , (b)  $\text{Fe}_{13}^+$ , and (c)  $\text{Fe}_{14}^+$ .

TABLE II. Natural atomic orbital populations in the lowest total energy states of  $\text{Fe}_{13}$  and  $\text{Fe}_{13}^+$ .

		$\text{Fe}_{13}, 2S = 44\mu_B$					
	Spin majority	OCC <sup>a</sup>	Spin minority	OCC <sup>a</sup>	Total	OCC <sup>a</sup>	
Central Fe	$3d^{4.93}4s^{0.44}4p^{0.04}4d^{0.13}$	5.54	$3d^{2.68}4s^{0.47}4p^{0.09}4d^{0.05}$	3.29	$3d^{7.61}4s^{0.91}4p^{0.13}4d^{0.18}$	8.83	
Apex Fe	$3d^{4.96}4s^{0.63}4p^{0.04}$	5.63	$3d^{1.93}4s^{0.30}4p^{0.03}$	2.26	$3d^{6.89}4s^{0.93}4p^{0.07}$	7.89	
Ring atoms	$3d^{4.96}4s^{0.69}4p^{0.04}$	5.69	$3d^{1.88}4s^{0.30}4p^{0.03}$	2.21	$3d^{6.84}4s^{0.98}4p^{0.07}$	7.90	
$\text{Fe}_{13}^+, 2S = 35\mu_B$							
Central Fe	$3d^{4.19}4s^{0.25}4p^{1.04}4d^{0.02}$	5.49	$3d^{3.88}4s^{0.27}4p^{1.05}4d^{0.03}$	5.23	$3d^{8.07}4s^{0.52}4p^{2.09}4d^{0.06}$	10.74	
Apex Fe	$3d^{4.92}4s^{0.20}4p^{0.16}$	5.28	$3d^{2.07}4s^{0.17}4p^{0.15}$	2.39	$3d^{7.00}4s^{0.37}4p^{0.31}$	7.68	
Ring atoms	$3d^{4.92}4s^{0.20}4p^{0.16}$	5.28	$3d^{2.07}4s^{0.17}4p^{0.15}$	2.39	$3d^{7.00}4s^{0.37}4p^{0.31}$	7.68	
$\Delta_{\text{Cat-Neutr}}^b$		-4.85		+4.0		+0.8	

<sup>a</sup>OCC denotes the total population of atomic valence orbitals. Small contributions from excited orbitals are omitted.

<sup>b</sup> $\Delta_{\text{Cat-Neutr}}$  is the difference between the total occupations from the top and bottom parts of the corresponding column.

populations in the lowest total energy states of  $\text{Fe}_{13}$  and  $\text{Fe}_{13}^+$ , which reflect their chemical bonding peculiarities. Table II presents the majority spin, minority spin, and total NAO populations of  $\text{Fe}_{13}$  and  $\text{Fe}_{13}^+$ . The total populations in the neutral  $\text{Fe}_{13}$  cluster are rather typical<sup>37</sup> and correspond to the promotion of a  $4s$  electron into the minority  $3d$  shell in the ground state  $3d^64s^2$  electronic configuration of a Fe atom (see the last column in Table II). In  $\text{Fe}_{13}^+$ , the  $4s$  atomic states are depleted because of their promotion not only into the minority  $3d$  shells, but also into  $4p$  states, which apparently are more accessible in positively charged species than in the corresponding neutrals. The net difference between the sums of the total occupations in  $\text{Fe}_{13}$  and  $\text{Fe}_{13}^+$  is  $0.8e$  instead of  $1.0e$  because of the discarded small populations of excited AOs.

Comparing the majority and minority spin populations, one can notice that the promotion of  $4s$  majority electrons into  $4p$  vacant orbitals of the surface and central atoms leads to the difference of  $-4.85e$  between the cation and the neutral majority spin populations. Note that  $0.15e$  that would be required to yield an integer number 5 is lost because the populations of higher excited orbitals are discarded for simplicity. On the contrary, the difference between the total minority spin populations of  $\text{Fe}_{13}^+$  and  $\text{Fe}_{13}$  is  $+4.0e$ . That is, the net change in the excess spin densities is  $9\mu_B$ .

It is natural to ask why such a significant  $4s \rightarrow 4p$  promotion, resulting in a large decrease in the total spin magnetic moment, is realized in  $\text{Fe}_{13}^+$ ? The answer is related to the high  $T_h$  symmetry of this cation wave function. The bonding orbitals, belonging to  $T_{1u}$  representation of the  $T_h$  point group, are composed of  $4p$  orbitals and accommodate six electrons. This special set of bonding orbitals makes the  $\text{Fe}_{13}^+$

cation thermodynamically more stable than any other cation in this size range. Our bonding energy of 4.00 eV, corresponding to the decay channel  $\text{Fe}_{13}^+ \rightarrow \text{Fe}_{12}^+ + \text{Fe}$ , compares well with the experimental value of  $4.02 \pm 0.47$  eV.<sup>38</sup>

In conclusion, density functional theory based calculations of the equilibrium geometries, total energies, and magnetic properties of  $\text{Fe}_n$  and  $\text{Fe}_n^+$  clusters ( $n = 12-14$ ) show that the computed total spin magnetic moments are in good agreement with recent experimental data. In particular, we reproduce the experimentally observed abrupt decrease in the total magnetic moment of  $\text{Fe}_{13}^+$ . The reason for this anomalous behavior is related to the fact that  $\text{Fe}_{13}^+$  has the  ${}^3A_u$  ground state of  $T_h$  symmetry, and this state possesses six occupied bonding orbitals of  $T_{1u}$  symmetry, which is unique for small size iron clusters. In order to fill these bonding orbitals, the majority spin  $4s$  electrons are to be promoted into the minority spin  $4p$  states. This process leads to the quenching of the magnetic moment at the central atom and is responsible for the exceptionally low value of the total magnetic moment in the  $\text{Fe}_{13}^+$  cation. It is worth noting that the dependence of the total spin magnetic moment on the symmetry of geometrical configurations in neutral  $\text{Fe}_{13}$  was studied earlier.<sup>21,39</sup> We should reiterate that the state  $2S = 31\mu_B$  where the magnetic moment of the central atom is coupled antiferromagnetically with the surface atoms is higher in total energy by +1.30 eV and cannot be the reason for the exceptionally low value of the total magnetic moment of  $\text{Fe}_{13}^+$  as hypothesized.

The work was partly supported by a grant from the Department of Energy.

\*Corresponding author: pjena@vcu.edu

<sup>1</sup>F. Liu, M. R. Press, S. N. Khanna, and P. Jena, *Phys. Rev. B* **39**, 6914 (1989); M. R. Press, F. Liu, S. N. Khanna, and P. Jena, *ibid.* **40**, 399 (1989).

<sup>2</sup>M. Castro, S.-R. Liu, H.-J. Zhai, and L.-S. Wang, *J. Chem. Phys.* **118**, 2116 (2003).

<sup>3</sup>S. E. Weber, B. K. Rao, P. Jena, V. S. Stepanyuk, W. Hergert, K. Wildberger, R. Zeller, and P. H. Dederichs, *J. Phys.: Condens. Matter* **9**, 10739 (1997).

<sup>4</sup>Y.-C. Bae, H. Osanai, V. Kumar, and Y. Kawazoe, *Phys. Rev. B* **70**, 195413 (2004).

<sup>5</sup>V. Kumar and Y. Kawazoe, *Eur. Phys. J. D* **24**, 81 (2003).

<sup>6</sup>M. Moseler, H. Häkkinen, R. N. Barnett, and U. Landman, *Phys. Rev. Lett.* **86**, 2545 (2001).

<sup>7</sup>B. V. Reddy, S. N. Khanna, and B. I. Dunlap, *Phys. Rev. Lett.* **70**, 3323 (1993); B. V. Reddy, S. K. Nayak, S. N. Khanna, B. K. Rao, and P. Jena, *Phys. Rev. B* **59**, 5214 (1999).

- <sup>8</sup>A. J. Cox, J. G. Louderback, and L. A. Bloomfield, *Phys. Rev. Lett.* **71**, 923 (1993).
- <sup>9</sup>L. A. Bloomfield, J. Deng, H. Zhang, and J. W. Emmert, in *Proceedings of the International Symposium on Cluster and Nanostructure Interface*, edited by P. Jena, S. N. Khanna, and B. K. Rao (World Scientific, Singapore, 2000), p. 131.
- <sup>10</sup>M. B. Knickelbein, *Phys. Rev. Lett.* **86**, 5255 (2001).
- <sup>11</sup>I. M. L. Billas, J. A. Becker, A. Châtelain, and W. A. de Heer, *Phys. Rev. Lett.* **71**, 4067 (1993).
- <sup>12</sup>I. M. L. Billas, A. Châtelain, and W. A. de Heer, *Science* **265**, 1682 (1994).
- <sup>13</sup>S. E. Apsel, J. W. Emmert, J. Deng, and L. A. Bloomfield, *Phys. Rev. Lett.* **76**, 1441 (1996).
- <sup>14</sup>R. A. Guirado-López, J. Dorantes-Dávila, and G. M. Pastor, *Phys. Rev. Lett.* **90**, 226402 (2003).
- <sup>15</sup>S. Sahoo, A. Hucht, M. E. Gruner, G. Rollmann, P. Entel, A. Postnikov, J. Ferrer, L. Fernández-Seivane, M. Richter, D. Fritsch, and S. Sil, *Phys. Rev. B* **82**, 054418 (2010).
- <sup>16</sup>M. Niemeyer, K. Hirsch, V. Zamudio-Bayer, A. Langenberg, M. Vogel, M. Kossick, C. Ebrecht, K. Egashira, A. Terasaki, T. Möller, B. v. Issendorff, and J. T. Lau, *Phys. Rev. Lett.* **108**, 057201 (2012).
- <sup>17</sup>G. L. Gutsev, M. Mochena, P. Jena, C. W. Bauschlicher, Jr., and H. Partridge III, *J. Chem. Phys.* **121**, 6785 (2004).
- <sup>18</sup>G. L. Gutsev and C. W. Bauschlicher, Jr., *J. Phys. Chem. A* **107**, 7013 (2003).
- <sup>19</sup>P. Bobadova-Parvanova, K. A. Jackson, S. Srinivas, and M. Horoi, *Phys. Rev. B* **66**, 195402 (2002).
- <sup>20</sup>O. Diéguez, M. M. G. Alemany, C. Rey, P. Ordejón, and L. J. Gallego, *Phys. Rev. B* **63**, 205407 (2001).
- <sup>21</sup>R. Singh and P. Kroll, *Phys. Rev. B* **78**, 245404 (2008).
- <sup>22</sup>G. L. Gutsev, C. A. Weatherford, P. Jena, E. Johnson, and B. R. Ramachandran, *J. Phys. Chem. C* **116**, 7050 (2012).
- <sup>23</sup>G. Rollmann, P. Entel, and S. Sahoo, *Comput. Mater. Sci.* **35**, 275 (2006).
- <sup>24</sup>M. J. Piotrowski, P. Piquini, and J. L. F. Da Silva, *Phys. Rev. B* **81**, 155446 (2010).
- <sup>25</sup>G. Kresse and J. Furthmüller, *Phys. Rev. B* **54**, 11169 (1996).
- <sup>26</sup>B. Delley, *J. Chem. Phys.* **92**, 508 (1990); **113**, 7756 (2000). DMOL<sup>3</sup> is available as part of Materials Studio software.
- <sup>27</sup>M. J. Frisch, G. W. Trucks, H. B. Schlegel, G. E. Scuseria, M. A. Robb, J. R. Cheeseman, G. Scalmani, V. Barone, B. Mennucci, G. A. Petersson, H. Nakatsuji, M. Caricato, X. Li, H. P. Hratchian, A. F. Izmaylov, J. Bloino, G. Zheng, J. L. Sonnenberg, M. Hada, M. Ehara, K. Toyota, R. Fukuda, J. Hasegawa, M. Ishida, T. Nakajima, Y. Honda, O. Kitao, H. Nakai, T. Vreven, J. A. Montgomery, Jr., J. E. Peralta, F. Ogliaro, M. Bearpark, J. J. Heyd, E. Brothers, K. N. Kudin, V. N. Staroverov, R. Kobayashi, J. Normand, K. Raghavachari, A. Rendell, J. C. Burant, S. S. Iyengar, J. Tomasi, M. Cossi, N. Rega, J. M. Millam, M. Klene, J. E. Knox, J. B. Cross, V. Bakken, C. Adamo, J. Jaramillo, R. Gomperts, R. E. Stratmann, O. Yazyev, A. J. Austin, R. Cammi, C. Pomelli, J. W. Ochterski, R. L. Martin, K. Morokuma, V. G. Zakrzewski, G. A. Voth, P. Salvador, J. J. Dannenberg, S. Dapprich, A. D. Daniels, Ö. Farkas, J. B. Foresman, J. V. Ortiz, J. Cioslowski, and D. J. Fox, GAUSSIAN 09, Revision B.01 (Gaussian, Inc., Wallingford, CT, 2009).
- <sup>28</sup>P. E. Blöchl, *Phys. Rev. B* **50**, 17953 (1994).
- <sup>29</sup>K. Raghavachari and G. W. Trucks, *J. Chem. Phys.* **91**, 1062 (1989).
- <sup>30</sup>A. D. Becke, *Phys. Rev. A* **38**, 3098 (1988).
- <sup>31</sup>J. P. Perdew and Y. Wang, *Phys. Rev. B* **45**, 13244 (1992).
- <sup>32</sup>J. P. Perdew, J. A. Chevary, S. H. Vosko, K. A. Jackson, M. R. Pederson, D. J. Singh, and C. Fiolhais, *Phys. Rev. B* **46**, 6671 (1992).
- <sup>33</sup>J. P. Perdew, K. Burke, and M. Ernzerhof, *Phys. Rev. Lett.* **77**, 3865 (1996).
- <sup>34</sup>E. K. Parks, T. D. Klots, and S. J. Riley, *J. Chem. Phys.* **92**, 3813 (1990).
- <sup>35</sup>S. Yang and M. B. Knickelbein, *J. Chem. Phys.* **93**, 1533 (1990).
- <sup>36</sup>M. B. Knickelbein, *Chem. Phys. Lett.* **353**, 221 (2002).
- <sup>37</sup>G. L. Gutsev and C. W. Bauschlicher, Jr., *J. Phys. Chem. A* **107**, 4755 (2003).
- <sup>38</sup>L. Lian, C.-X. Su, and P. B. Armentrout, *J. Chem. Phys.* **97**, 4072 (1992).
- <sup>39</sup>H. M. Duan and Q. Q. Zheng, *Phys. Lett. A* **280**, 333 (2001).